JPE 16-2-38

http://dx.doi.org/10.6113/JPE.2016.16.2.798
ISSN(Print): 1598-2092 / ISSN(Online): 2093-4718

A Control Method for Power-Assist Devices using a BLDC Motor for Manual Wheelchairs

Dong-Youn Kim*, Yong-Hyu Kim**, Kwang-Sik Kim***, and Jang-Mok Kim†

*,†Department of Electrical Engineering, Pusan National University, Busan, Korea
**Busan Techno Park, Busan, Korea
***LG Electronics, Changwon, Korea

Abstract

This paper proposes a new operation and control strategy for Power-Assisted Wheelchairs (PAW) using one brushless DC (BLDC) motor. The conventional electrical wheelchairs are too heavy and large for one person to move because they have two electric motor wheels. On the other hand, the proposed PAW system has a small volume and is easy to move due to the presence of a single wheel motor. Unlike the conventional electric wheelchairs, this structure for a PAW does not have a control joystick to reduce its weight and volume. To control the wheelchair without a joystick, a special control system and algorithm are needed for proper operation of the wheelchair. In the proposed PAW system uses only one sensor to detect the acceleration and direction of PAW's movement. By using this sensor, speed control can be achieved. With a speed control system, there are three kinds of operations that can be done on the speed of a PAW: the increment of PAW speed by summing external force, the decrement of PAW speed by subtracting external force, and emergency breaking by evaluating the time duration of external force. The validity of the proposed algorithm is verified through experimental results.

Key words: Assist equipment, Brushless DC motor, Power-assisted wheelchair sensor, Speed control, Wheelchair control

I. Introduction

In recent years, elderly and disabled people have become more active in social activities due in part to the development of medical and electric technology. The areas of activity for these people are wider than they were a decade ago. Electric wheelchairs are usually used for short distance movement while cars are required for the movement of electric wheelchairs over a long distance. However, conventional wheelchairs which have joysticks are too heavy and large to load into a car alone. Some PAWs have been developed to achieve light weight and portability from manual wheelchair [1]-[9]. These PAWs are not equiped with joysticks and use torque sensors or acceleration sensors to measure or estimate the speed or acceleration which is generated by the pushing power of the user. Pushing power is used for the propulsion of manual wheelchairs. For the most part, there are two types of PAW systems. One is the systems having two motors connected with both wheels of the wheelchair. In this type of PAW, since the PAW is already installed on the wheelchair, there is no need for the user to install it. However, it is difficult to repair once it is damaged. The second type is the attachable power assist device (PAD), where attachable and portable hardware is attached to a wheelchair whenever the user wants to use the PWA system. Attachable PADs can be simply applied to several manual wheelchairs.

The conventional studies on PAWs focused on the use of two motors. These PAW systems use pushing power to generate the assist power. Because assist power is temporarily added for propulsion, a number of propulsion motions (pushing wheels) are required to continuously move the wheelchair. However, excessive propulsion motions have a bad effect on wrist joints [10]. In addition, the installation of two motors causes a weight increment. Therefore, the user needs considerable force to load or unload a wheelchair into or out of a car.

In this paper, a different control algorithm is proposed and compared to the conventional PAW control algorithm. The concept of the proposed algorithm is that the wheelchair

Manuscript received Apr. 6, 2015; accepted Oct. 5, 2015
Recommended for publication by Associate Editor Kwang-Woon Lee.
†Corresponding Author: jmok@pusan.ac.kr
Tel: +82-51-510-2366, Fax: +82-51-513-0212, Pusan Nat'l University
*Dept. of Electrical Eng., Pusan National University, Korea
**Busan Techno Park, Korea
***LG Electronics. Korea

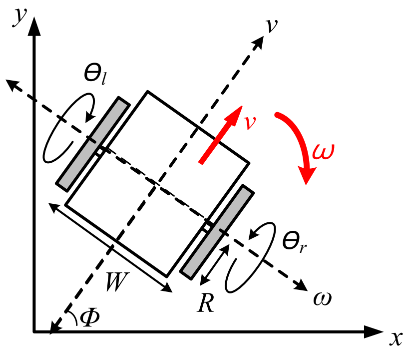

Fig. 1. Electrical wheelchair model.

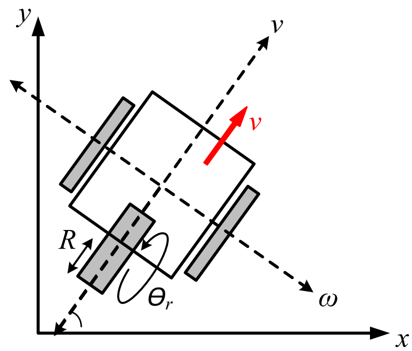

Fig. 2. Proposed PAW wheelchair model.

can maintain speed for a long time with a single pushing action. It helps the user move a long way without applying a lot of pushing actions. This proposed control algorithm uses one acceleration sensor. The control algorithm is composed of three control methods. One is the accumulation of the speed command to increase the speed of the wheelchair. The second method is the deceleration of the speed command to decrease speed of the wheelchair. The third is the quick stop control for emergency situations. These algorithms are based on the output of the acceleration sensor and are combined for speed control. The proposed algorithm is verified by experimental results.

II. MODELING OF THE PROPOSED PAW WHEELCHAIR

A. Conventional Model of a Wheelchair Controlled by Two Wheels [11]

Fig. 1 shows the conventional model of a wheelchair. The wheel chair model has two domains which are the propulsion and rotation, where v is the propulsion speed, and ω is the rotational speed. The kinematics of the wheelchair can be represented as (1) and (2).

$$v = \frac{R}{2}\left(\dot{\theta}_l + \dot{\theta}_r\right) \tag{1}$$

$$\omega = \frac{R}{W}\left(\dot{\theta}_l - \dot{\theta}_r\right) \tag{2}$$

where $\dot{\theta}_l, \dot{\theta}_r$ are the angular speeds of the left and right wheels, ϕ is the moving direction, R is the radius of the wheel, and W is the distance between the two wheels.

Then, the time derivative of (1) and (2) can be represented as follows.

$$\dot{v} = \frac{R}{2}\left(\ddot{\theta}_l + \ddot{\theta}_r\right) \tag{3}$$

$$\dot{\omega} = \frac{R}{W}\left(\ddot{\theta}_l - \ddot{\theta}_r\right) \tag{4}$$

The propulsion force and rotation torque of the wheelchair can be expressed as (5) and (6).

$$F_p = m\dot{v} = m\frac{R}{2}\left(\ddot{\theta}_l + \ddot{\theta}_r\right) \tag{5}$$

$$T_r = J\ddot{\phi} = J\frac{R}{W}\left(\ddot{\theta}_l - \ddot{\theta}_r\right) \tag{6}$$

To derive the motion equation of the wheelchair, the total kinetic energy of the wheelchair L is given by equation (7).

$$L = \frac{1}{2}\frac{mR^2}{4}(\dot{\theta}_l + \dot{\theta}_r)^2 + \frac{1}{2}J(\frac{R}{W}(\dot{\theta}_l - \dot{\theta}_r))^2 + \frac{1}{2}J_\omega(\dot{\theta}_l{}^2 + \dot{\theta}_r{}^2) \tag{7}$$

Solving the Lagrange equation, the load torque equation of the wheelchair can be presented as (8).

$$\begin{bmatrix} \tau_r \\ \tau_l \end{bmatrix} = \begin{bmatrix} \frac{mR^2}{4} + \frac{JR^2}{W^2} + J_\omega & \frac{mR^2}{4} - \frac{JR^2}{W^2} \\ \frac{mR^2}{4} - \frac{JR^2}{W^2} & \frac{mR^2}{4} + \frac{JR^2}{W^2} + J_\omega \end{bmatrix} \begin{bmatrix} \ddot{\theta}_r \\ \ddot{\theta}_l \end{bmatrix} + B_w \begin{bmatrix} \dot{\theta}_r \\ \dot{\theta}_l \end{bmatrix} \tag{8}$$

where, m and J are the mass and inertia of the wheelchair, and J_ω and B_ω are the inertia and friction coefficient of the wheel, respectively.

B. Model of the Proposed PAW Wheelchair

Fig. 2. shows the proposed model using one propulsion motor. In this case, the motor can control only the propulsion force. That means the rotational force can be neglected, that is θ_l and θ_r are equal. The kinematics of the proposed wheelchair can be represented as (9) and (10).

$$v = R\dot{\theta} \tag{9}$$

$$\dot{v} = R\ddot{\theta} \tag{10}$$

where, $\dot{\theta}$ and $\ddot{\theta}$ are the angular speed and acceleration speed of the propulsion motor.

The propulsion force is replaced by (11), and the total kinetic energy of the proposed wheelchair L is given by equation (12).

$$F_p = m\dot{v} = mR\ddot{\theta} \tag{11}$$

$$L = \frac{mR^2}{2}\dot{\theta}^2 + \frac{J_\omega}{2}\dot{\theta}^2 \tag{12}$$

Finally, the load torque equation of the proposed wheelchair can be derived as (13).

$$\tau = mR^2\ddot{\theta} + J_\omega\ddot{\theta} + B_\omega\dot{\theta} \tag{13}$$

III. Proposed Power Assist Device Control Algorithm

A. Maximum Speed Tracking and Keeping Algorithm

In the proposed PAW, an acceleration sensor is used to detect the external force applied by the user. The output of the acceleration sensor is converted to the additional speed, v_h, which is used for the generation of the speed command of the proposed PAW system.

The acceleration sensor has a positive value when the user pushes the wheelchair wheels in the positive direction as shown in Fig. 3. Fig. 3 shows the direction of the additional speed and acceleration when a positive direction external force is applied, where a_h is the acceleration measured by the acceleration sensor, and v_h is the additional speed produced by an external force. v_h can be calculated by integrating the acceleration as given by equation (14).

$$v_h = \int_0^t a_h dt \tag{14}$$

This additional speed can be added to or subtracted from the real wheelchair speed, v.

Fig. 4 shows the profile of ah and vh. When the user pushes the wheelchair wheels, ah can be measured through the acceleration sensor. Following the profile of ah, the real velocity of the wheelchair increases. However, the speed of the wheelchair steadily decrease due to frictional force. The external force makes the additional speed profile vh like the half cycle of a sine waveform. From the profile, assisted-speed va can be generated from vh by using equation (15). It is not suitable to adapt vh as a speed command from the acceleration sensor output since it has a lot of noise and a small magnitude. Thus, the scale and slope of va can be controlled by using equation (15).

$$v_a = \frac{K_a}{1+\tau_a s} v_h \tag{15}$$

where, v_a is the assisted-speed, K_a is the assistance coefficient, and τ_a is the time constant.

To drive continuously by applying only one propulsion motion, the maximum value is retained for the calculation of the speed command. The speed command v_a^* can be acquired by using the differential value of v_a to detect the maximum speed value. Fig. 4 schematically shows the above mentioned explanations of the mechanism used to detect the maximum speed point. According to the differential value of v_a, the speed command v_a^* can be presented like equation (16)

$$v_a{}^* = \begin{cases} v_a & v_a - v_{a\_old} \geq 0 \\ v_{a\_max} = v_{a\_old} & v_a - v_{a\_old} < 0 \end{cases} \tag{16}$$

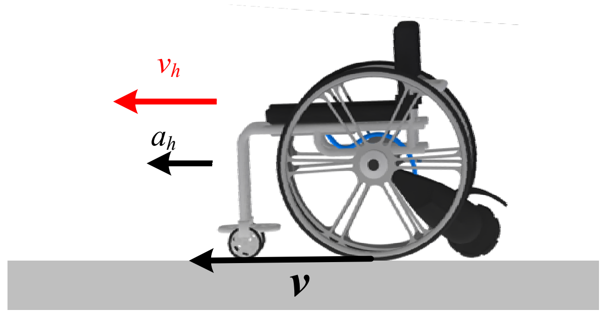

Fig. 3. Movement of Power-Assisted Wheelchair.

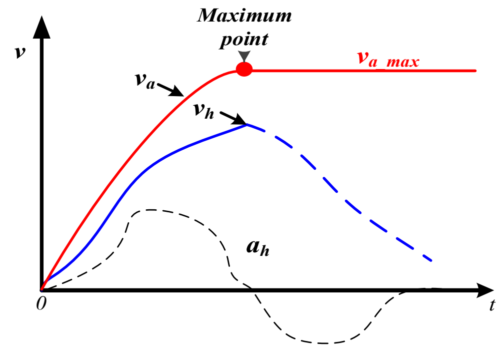

Fig. 4. Profile of acceleration sensor and detecting maximum speed to keep constant speed for PAW.

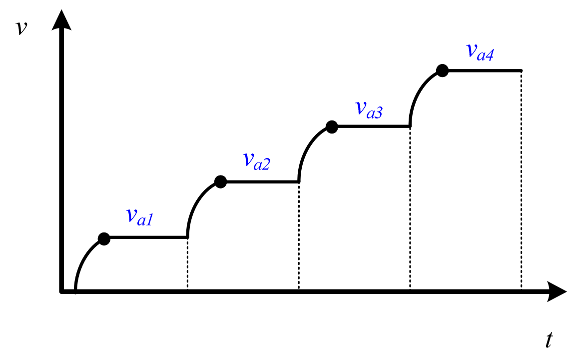

Fig. 5. Summation of speed by adding the external force.

where v_{a_old} is the value of v_a calculated before a period of time.

B. Algorithm for Increasing the Speed Command

In the proposed PAW system, the speed of the wheelchair can be changed according to the magnitude and direction of the external force. Therefore, the speed command can be determined by summing the number of the external forces according to the drive direction as v_{a1}, v_{a2}, v_{a3} and v_{a4} which are determined by each external force as shown in Fig. 5. This means that whenever an external positive force is applied, the speed command increases to the next level as depicted in Fig. 5.

C. Braking Algorithm

A braking algorithm must be included in the proposed system unlike conventional electric wheelchairs with a joystick or PAW based torque controls.

There are two steps in the proposed braking algorithm. Firstly, the brake ratio is decided according to the time duration. Then, the braking method is decided since there are two braking methods. One is the deceleration in case of a decrement in the speed command following the decided brake ratio. Another is a quick stop if the user wants to reduce the speed command quickly.

The braking motion is activated by grasping the wheelchair wheel. In this case, the profile time of the deceleration is the reference signal of the braking as shown in Fig. 6 and Fig. 7, respectively.

Fig. 6 shows the direction of the additional speed and the acceleration of the wheelchair during the braking operation. The acceleration has a negative value in accordance with the driving direction.

Fig. 7 shows the acceleration pattern in case of the braking operation of the wheelchair. To avoid the effects of noise, the brake signal is recognized after a few seconds from the point where grasping of the wheel occurs.

In Fig. 7, t_1 is the point where grasping the wheelchair wheels for braking occurs. It is decided that the acceleration signal goes down under zero. t_2 is the point of distinction for brake mode: speed decrement or complete break. The distinction is made up with the speed error and acceleration signal. If the user grips the rim strongly, the speed error reaches the distinction point in a short time. Otherwise, if the user grips the rim smoothly and continuously, the speed error gently increases to the distinction point over a long time. The distinction time is experimentally defined to be 15% of the speed commands. Thus, T_{br} is the detection time between t_1 and t_2 and it is related to the brake ratio. The brake ratio determines the decremental ratio of the speed command. If T_{br} is short, it means that the user wants to quickly reduce the speed command.

Fig. 8 shows the speed command according to T_{br} and the brake ratio. The variables α is used for the division of T_{br}. If T_{br} has an arbitrary value between 0 and α, as in Fig. 8(a), it can be considered that the user wants to stop quickly. In this case, the brake ratio is determined to be a large value. If T_{br} is longer than α, as shown in Fig. 8(b), the brake ratio is determined to have a small value and α is set by the acceleration profile.

After the brake ratio is determined, T_{stop} is used for selecting the deceleration or quick stop of the wheelchair. T_{stop} is the elapsed time between t_2 and t_3. If the user grasps the wheel for a moment, the speed is reduced for a short time and the speed again follows the speed command.

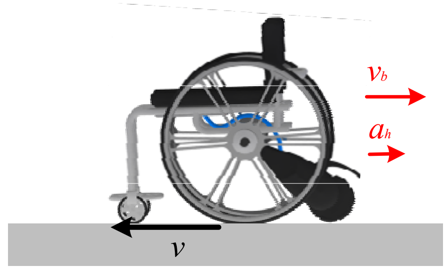

Fig. 6. The velocity and acceleration during deceleration/stop.

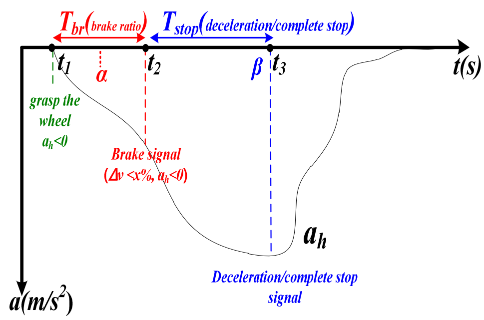

Fig. 7. Acceleration during reduction of speed.

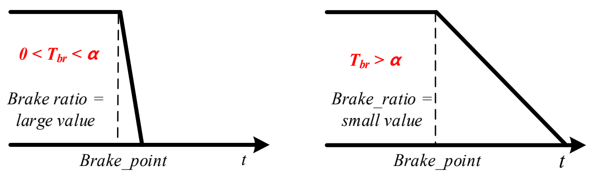

(a) (b)

Fig. 8. Speed command according to the brake ratio. (a) Large brake ratio. (b) Small brake ratio.

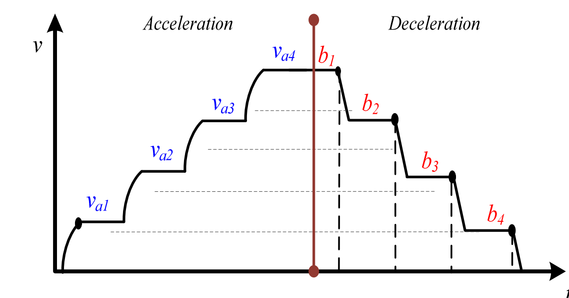

(a) Speed command with the acceleration and deceleration.

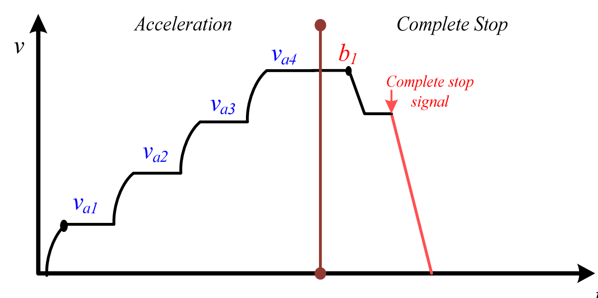

(b) Speed command with the acceleration and quick stop.

Fig. 9. Speed command about two cases of brake.

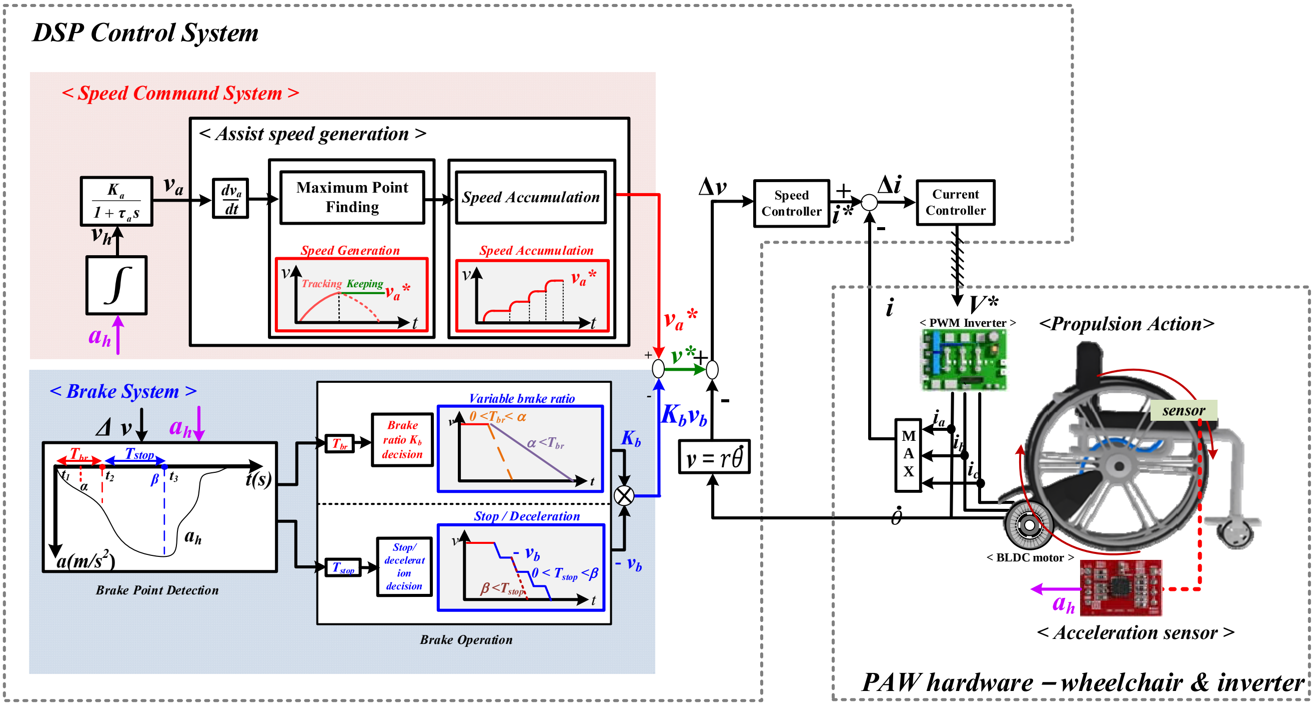

Fig. 10. Whole block diagram of the proposed control algorithm.

In this case, the acceleration acquires negative value for a moment. However, if the user grasps the wheel for a long time, the speed of the wheelchair is reduced continuously. In this case, the acceleration has negative value for a long time. If T_{stop} is longer than β, the system will decide to quick stop the wheelchair. Otherwise, it can be considered to be a deceleration of the speed command.

The deceleration operation is implemented in stages like the increasing operation of the speed command. As shown in Fig 9(a), the speed command is reduced in stages during the deceleration operation. The quick stop operation is used for quick stops in case of an emergency. Once the brake signal occurs, the first stage of deceleration is implemented. As shown in Fig. 9(b), the quick stop signal is generated during the first deceleration step.

IV. EXPERIMENTAL RESULTS

Fig. 10 shows a whole block diagram of the proposed algorithm. The proposed PAW system is composed of a DSP control system, a manual wheelchair and a PAW hardware system. The acceleration generated by an external force is used as the speed command for the DSP control system, and the system keeps the speed command steadily. If additional acceleration occurs during the speed control, the speed command increases in step. When the braking motion is detected, the brake-command ($K_b v_b$) is subtracted from the speed command (v_a^*). Then, the final speed-command (v^*) is used as the reference speed for the DSP control system.

(a) Configuration of PAW (b) Backside of Wheelchair

Fig. 11. Configuration of wheelchair.

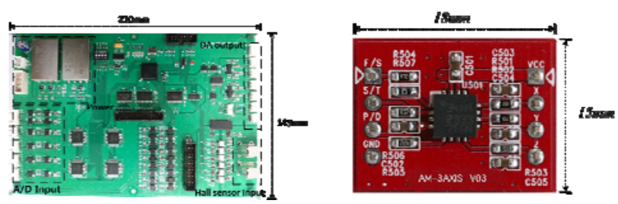

(a) (b)

Fig. 12. DSP control board and acceleration sensor. (a) DSP control board used for the experiment. (b) Acceleration sensor AM-3AXIS V03.

Fig. 11(a) shows the configuration of the wheelchair on which the power assist device is installed. Fig. 11(b) shows the backside of the wheelchair with the PAD. The power rating of the motor is 300(W).

Fig. 12(a) shows a control board which uses a TMS320F335 as the main processor [12]. The acceleration sensor for the proposed algorithm is represented in Fig. 12(b). The sensor is a AM-3AXIS of STMicroelectronics [13] and experimental data are logged by a NI DAQPAD-6251.

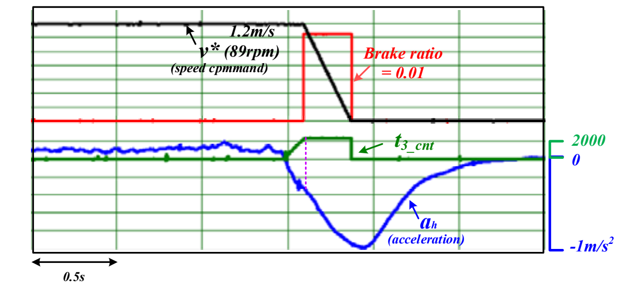

Fig. 13. Quick stop operation when Brake ratio = 0.01.

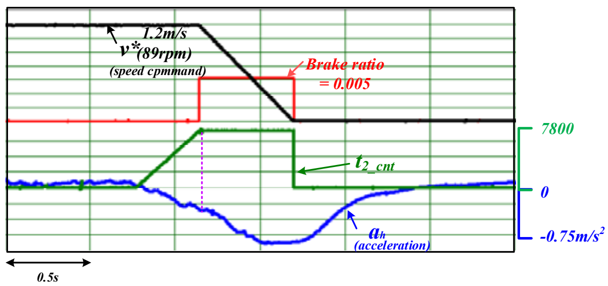

Fig. 14. Quick stop operation when Brake ratio = 0.005.

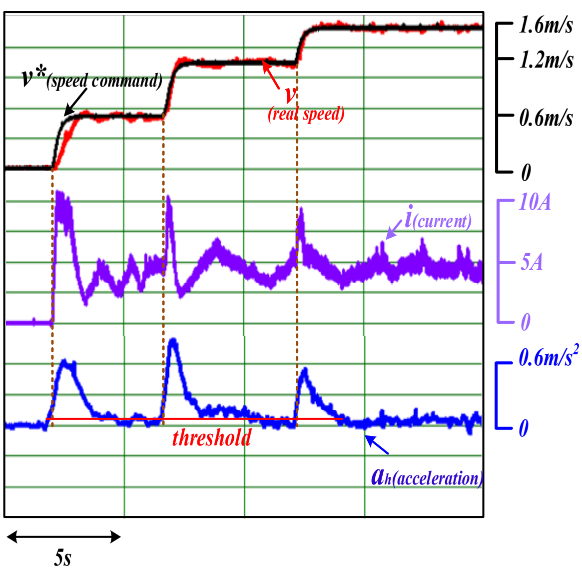

Fig. 15. Experimental results of the continuous increment of the speed.

Fig. 13 and Fig. 14 show experimental results of the brake ratio according to T_{br}. In the experiment, α is 0.5s. The T_{br} counter counts every 100us. As shown in Fig. 13, the brake ratio is determined to have a large value when T_{br} is shorter than 0.5s. As shown in Fig. 14, the brake ratio has a small value because T_{br} is longer than 0.5s.

Fig. 15 shows experimental result of the continuous propulsion operation. To avoid malfunctions caused by noise, the propulsion motion is recognized when the output of the sensor is larger than a threshold value. In this experiment, the maximum speed is limited to 1.6m/s for the sake of safety, and the speed of each stage is 0.6 m/s. To track the speed

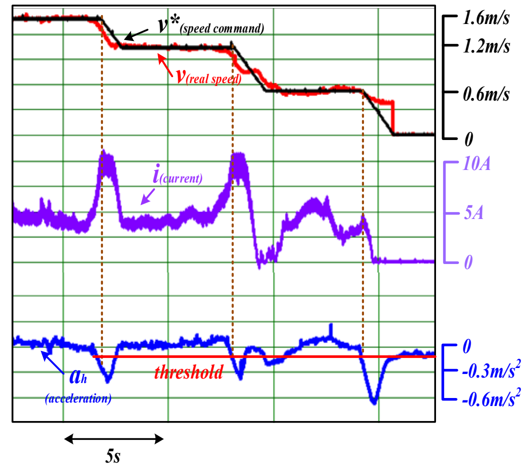

Fig. 16. Experimental results of the continuous decrement of the speed.

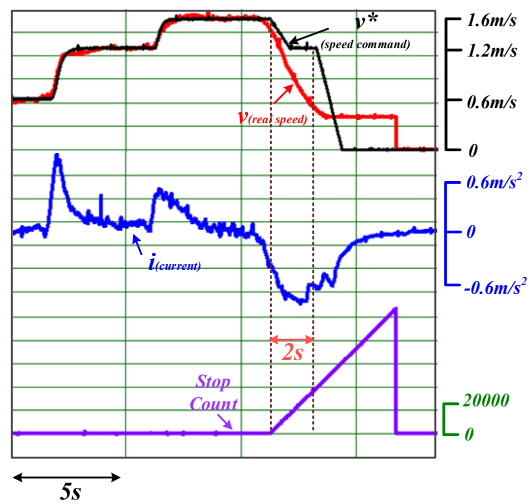

Fig. 17. Experimental result of the quick stop of the speed.

command (v^*), the current increases during the transient state, and the current is maintained at a fixed speed.

Fig. 16 shows a waveform during the continuous deceleration operation of the wheelchair. To avoid malfunctions, the brake point is recognized when the acceleration is lower than the threshold. The current (i) increases during the deceleration operation. The reason is that a motion which grasps the wheelchair wheel is considered as an increase of the load condition until the controller recognizes the brake point.

Fig. 17 shows a waveform during quick the stop operation. In the experiment, the signal of the quick stop is generated when the acceleration (a_h) has negative value for more than two seconds (β=2s) from the starting point of the first deceleration step. In Fig. 15, the stop count increases every 100us. If the stop count equals to 20000, the speed command is reduced to zero directly. The real speed (v) cannot follow the speed command (v^*) because the user grasps the wheelchair wheels to reduce the speed.

V. CONCLUSION

In this paper, new operation and control strategies for the PAW of a manual wheelchair was proposed. The motion recognition was implemented in the PAW control system by the detection of the acceleration sensor output signal. The speed of the wheelchair was increased step by step according to external force applied by the user. In the brake operation, the user reduces the speed step by step or quickly and the controller determines whether the step by step or quick speed reduction is required according to the time duration of the acceleration. The validity of the proposed algorithm was verified through experimental results.

APPENDIX

Motor Data

Stator Resistor	0.25 [Ω]
Stator Inductance	565[uH]
Rated output power	300[W]
Rated current	9[A]
Rated voltage	36[V]
Number of poles	60

Wheelchair Data

Wheelchair Dimension (L x W x H)	590 x 950 x 850[mm]
Wheelchair weight	15.5[kg]
Wheel radius	0.13[m]
Power Assist Device Dimension	430 x 330 x 180[mm]
Power Assist Device Weight	17.8[kg]

ACKNOWLEDGMENT

This research was financially supported by the INNOPOLIS Foundation (14BSI388)

REFERENCES

[1] H. Seki, T. Sugimoto, and S. Tadakuma, “Novel straight road driving control of power assisted wheelchair based on disturbance estimation and minimum jerk control,” in *Industry Applications Conference*, Vol. 3, pp. 1711-1717, Oct. 2005.

[2] P.-W. Hsueh, M.-C. Tsai, H.-T. Pan, and A. Grandjean “Integrated synchronized motion control for a force sensorless power-assisted wheelchair,” in *Preprints of the 18th IFAC World Congress*, Vol. 18, pp. 5956-5961, Aug./Sep. 2011.

[3] Y. Munakata, A. Tanaka, and M. Wada, “An active-caster drive system for motorizing a manual wheelchair,” in *IEEE International Conference on Mechatronics and Automation(ICMA)*, pp. 1161-1166, Aug. 2013.

[4] D. K. Jones, R. A. Cooper, S. Albright, and M. Digiovine, “Power wheelchair driving performance using force and position sensing joysticks,” in *Proc. IEEE Bioengineering Conference*, pp. 130-132, Apr. 1998.

[5] Y. Oonishi, S. Oh, and Y. Hori, “A new control method for power-assisted wheelchair based on the surface myoelectric signal,” *IEEE Trans. Ind. Electron.*, Vol. 57, No. 9, pp. 3191-3196, Sep. 2010.

[6] C. Ou, C. Chen, and T. Chen, “Modeling and Design a Power Assisted Wheelchair used Torque Observer,” in *International Symposium on Computer Communication Control and Automation*, Vol. 2, pp. 63-66, May 2010.

[7] Y. Munnakata, A. Tanaka, and M. Wada, “A five-wheel wheelchair with an active-caster drive system,” in *IEEE International Conference on Rehabilitation Robotics (ICORR)*, pp. 1-6, Jun. 2013.

[8] S.-W. Hwang, C.-H. Lee, and Y.-B. Bang, “Power-assisted wheelchair with gravity compensation,” in *12th International Conference on Control, Automation and Systems(ICCAS)*, pp. 1874-1877, Oct. 2012.

[9] H. Seki and N. Tanohata, “Fuzzy control for electric power-assisted wheelchair driving on disturbance roads,” *IEEE Trans. Syst., Man, Cybern., Part C: Applications and Reviews*, Vol. 42, No. 6, pp. 1624-1632, Nov. 2012.

[10] I. Uriostegui, F. Bernal, J. A. Tover, E. Vela, M. Bourdon, and A. I. Perez, “Biomechanical analysis of the propulsion of the manual wheelchair in patients with spinal cord injury,” in *Pan American Health Care Exchanges (PAHCE)*, pp. 1-5, Apr. 2014.

[11] J. Miyata, Y. Kaida, and T. Murakami, “v–$\dot{\varphi}$-coordinate-based power-assist control of electric wheelchair for a caregiver,” *IEEE Trans. Ind. Electron.*, Vol. 55, No. 6, pp. 2517-2524, Jun. 2008.

[12] *TMS320F28335 data manual*, Texas Instrument, 2007.

[13] *LIS344ALH Datasheet*, STMicroelectronics, 2008.

Dong-Youn Kim was born in Ulsan, Korea, in 1983. He received his B.S. and M.S. degrees in Electrical Engineering from Pusan National University, Busan, Korea, in 2011 and 2013, respectively, where he is presently working towards his Ph.D. degree. His current research interests include power conversion, electric machine drives, and electrical vehicle propulsion.

Yong-Hyu Kim received his B.S. from Kunsan National University, Gunsan, Korea, in 2004; and his M.S. degree from the radio science engineering, Chungnam National University, Daejeon, Korea in 2012. He is working toward the Ph.D. degree in Electrical Engineering from Pusan National University, Busan, Korea. From 2005 to 2008, he was an associate research engineer at Korea Automotive Technology Institue (KATECH). Since 2008, he has been research engineer of automotive parts technology support center at the Busan techno park. His current research includes component of electrical vehicle.

Kwang-Sik Kim was born in Busan, Korea, in 1988. He received his M.S. degree in Electrical Engineering from Pusan National University, Busan, Korea, in 2015. He is currently working for LG Electronics, Changwon, Korea. His current research interests include electric machine drives in home appliances, and electrical vehicle propulsion.

Jang-Mok Kim received his B.S. from Pusan National University (PNU), Busan, Korea, in 1988; and his M.S. and Ph.D. degrees from the Department of Electrical Engineering, Seoul National University (SNU), Seoul, Korea, in 1991 and 1996, respectively. From 1997 to 2000, he was a Senior Research Engineer with the Korea Electrical Power Research Institute (KEPRI), Daejeon, Korea. Since 2001, he has been with the School of Electrical Engineering, PNU, where he is presently a Research Member in the Research Institute of Computer Information and Communication, a Faculty Member, and a head of the LG Electronics Smart Control Center. As a Visiting Scholar, he joined the Center for Advanced Power Systems (CAPS), Florida State University, Tallahassee, Florida, in 2007. His current research interests include the control of electric machines, electric vehicle propulsion, and power quality.